Earth and Planetary Science Letters 401 (2014) 183–195

Contents lists available at ScienceDirect

Earth and Planetary Science Letters

www.elsevier.com/locate/epsl

# Eocene rotation of Sardinia, and the paleogeography of the western Mediterranean region

Eldert L. Advokaat [a,b,*], Douwe J.J. van Hinsbergen [a], Marco Maffione [a], Cor G. Langereis [a], Reinoud L.M. Vissers [a], Antonietta Cherchi [c], Rolf Schroeder [d], Haroen Madani [a], Stefano Columbu [c]

[a] Department of Earth Sciences, Utrecht University, Budapestlaan 4, 3584 CD Utrecht, The Netherlands
[b] SE Asia Research Group, Department of Earth Sciences, Royal Holloway University of London, Egham, Surrey, TW20 0EX, United Kingdom
[c] Dipartimento di Scienze Chimiche e Geologiche, Università degli Studi di Cagliari, Via Trentino 51, I-09127 Cagliari, Italy
[d] Forschungsinstitut Senckenberg, Senckenberg-Anlage 25, D-60325 Frankfurt am Main, Germany

ARTICLE INFO

*Article history:*
Received 4 March 2014
Received in revised form 28 May 2014
Accepted 8 June 2014
Available online xxxx
Editor: Y. Ricard

*Keywords:*
Sardinia
Corsica
Briançonnais
Iberia
paleomagnetism

ABSTRACT

Key to understanding the complex Mediterranean subduction history is the kinematic reconstruction of its paleogeography after Jurassic extension between Iberia, Eurasia, and Africa. While post-Eocene Liguro-Provençal back-arc extension, and associated Miocene ~50° counterclockwise (ccw) rotation of Sardinia–Corsica have been well documented, pre-Oligocene reconstructions suffer uncertainties related to the position of Sardinia–Corsica with respect to Iberia. If a previously constrained major post-middle Jurassic, pre-Oligocene rotation of Sardinia–Corsica can be quantified in time, we can test the hypothesis that Sardinia–Corsica was (or was not) part of Iberia, which underwent a ~35° ccw during the Aptian (121–112 Ma). Here, we present new paleomagnetic results from Triassic, Jurassic, Upper Cretaceous and Lower Eocene carbonate rocks from Sardinia. Our results show a consistent well constrained post-early Eocene to pre-Oligocene ~45° ccw rotation of Sardinia–Corsica relative to Eurasia. This rotation postdated the Iberian rotation, and unambiguously shows that the two domains must have been separated by a (transform) plate boundary. The Eocene rotation of Sardinia–Corsica was synchronous with and likely responsible for documented N-S shortening in the Provence and the incorporation of the Briançonnais continental domain, likely connected to Corsica, into the western Alps. We argue that this rotation resulted from the interplay between a southward 'Alpine' subduction zone at Corsica, retreating northward, and a northward subduction zone below Sardinia, remaining relatively stationary versus Eurasia.



## 1. Introduction

Accurate kinematic reconstruction of Corsica and Sardinia since Jurassic extension between Iberia, Eurasia and Africa associated with the break-up of Pangea and the opening of the Central Atlantic ocean (Frisch, 1979; Rosenbaum et al., 2002a; Stampfli et al., 2002; Stampfli and Hochard, 2009; Speranza et al., 2012; Vissers et al., 2013), is key to restore the Cretaceous and younger subduction zone configuration and evolution of the western Mediterranean region. It is well established that since the Early Oligocene, Corsica and Sardinia were in an overriding plate position of the Apennine subduction zone and rifted away from southern France, opening the Liguro-Provençal back-arc extension in its wake (Malinverno and Ryan, 1986; Rosenbaum et al., 2002b; Faccenna et al., 2004; Jolivet et al., 2009; Handy et al., 2010; van Hinsbergen et al., 2014). This was associated with a rapid, Early Miocene 50° counterclockwise (ccw) vertical axis rotation of Sardinia–Corsica (Speranza et al., 2002; Gattacceca et al., 2007). Kinematic reconstructions for the Mesozoic to Eocene history of the central Mediterranean region are widely divergent, and hinge on whether Sardinia–Corsica was part of Eurasia, attached to the Provence in southern France, or part of Iberia.

This debate may be solved by paleomagnetic analysis. Previous paleomagnetic results from Middle Jurassic rocks of Sardinia (Horner and Lowrie, 1981; Kirscher et al., 2011) show that prior to the Miocene rotation, an additional ~40° ccw rotation must have occurred at an ill-defined stage in the Late Mesozoic or

* Corresponding author at: SE Asia Research Group, Department of Earth Sciences, Royal Holloway University of London, Egham, Surrey, TW20 0EX, United Kingdom.
*E-mail address:* e.l.advokaat@gmail.com (E.L. Advokaat).

http://dx.doi.org/10.1016/j.epsl.2014.06.012
0012-821X/

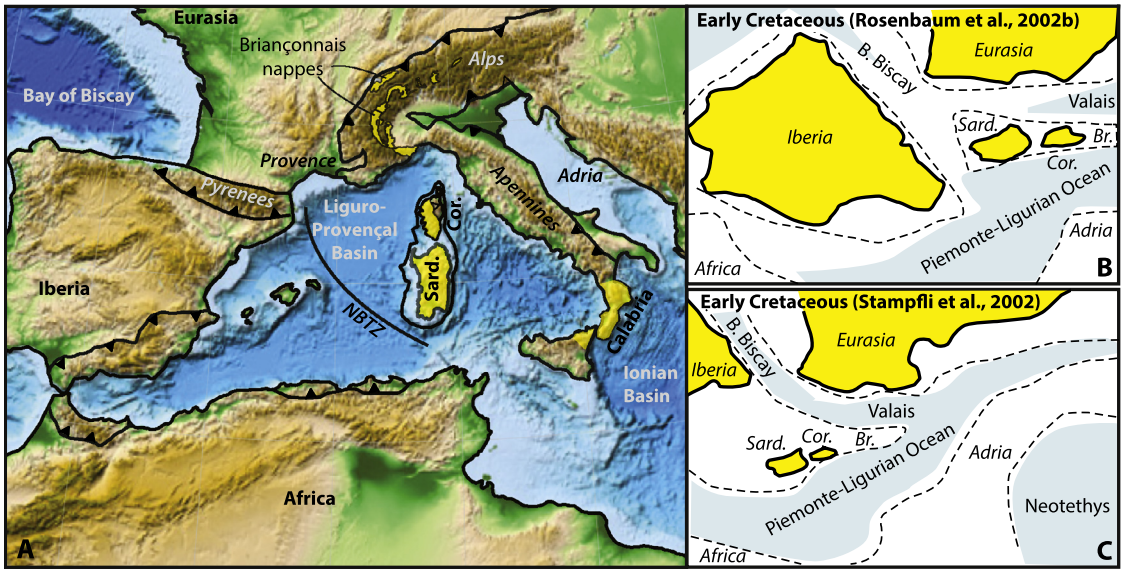


**Fig. 1.** (A) Map of the present-day geological setting of the central-western Mediterranean region. (B, C) Leading paleogeographic hypothesis for the paleogeography of the western Mediterranean region in the Early Cretaceous assuming that Sardinia–Corsica–Briançonnais (Sard., Cor., Br.) (B) was decoupled from and moved independent from Iberia (Rosenbaum et al., 2002b) or (C) was a part of rigid Iberia (Stampfli et al., 2002; Turco et al., 2012). NBTZ = North Balearic Transform Zone.

Paleogene, from which interval no paleomagnetic data are available from Sardinia or Corsica. Kirscher et al. (2011) suggested that this pre-Miocene rotation represented the well-documented Aptian–early Albian (~121–110 Ma) ~35° ccw rotation of Iberia (Van der Voo, 1969; Gong et al., 2008) and thus implied that Sardinia–Corsica were part of the Iberian continent (Fig. 1C), similar to reconstructions of e.g., Stampfli et al. (2002), Handy et al. (2010), and Turco et al. (2012). Conversely, Horner and Lowrie (1981) argued that Sardinia–Corsica was an independent microcontinent during the Mesozoic and early Cenozoic, located adjacent to the Provence (Fig. 1B), similar to reconstructions of e.g. Rosenbaum et al. (2002b).

In this paper, we aim to date the post-Middle Jurassic to pre-Miocene rotation phase of Sardinia, and test whether this coincided with, or postdated the Iberia rotation. Therefore we conducted an extensive paleomagnetic analysis of Triassic, Jurassic, Lower and Upper Cretaceous and Lower Eocene carbonate rocks from Sardinia. The implications of our results are integrated in the paleogeographic and kinematic evolution of the Mediterranean region.

## 2. Geological setting

Orogenesis in the central-western Mediterranean resulted from plate convergence between the Eurasian and African plates. This convergence was not only accommodated by subduction of oceanic crust, but also by the collision of microcontinental fragments that intervened ocean basins. This complex paleogeography resulted from an early to middle Mesozoic extension history at the junction between the Atlantic spreading system to the west and the Neotethyan ocean basin to the east. Neotethyan extension occurred during the Triassic, relics of which are found in the modern Ionian Basin. The Atlantic spreading system linked in Jurassic time to a now completely subducted ocean basin known as the Piemonte-Ligurian Ocean along the eastern margin of Iberia and the southern margin of Eurasia (Frisch, 1979; Rosenbaum et al., 2002a; Stampfli et al., 2002; Schmid et al., 2004; Stampfli and Hochard, 2009; Handy et al., 2010; Speranza et al., 2012; Vissers et al., 2013). The geology of the western Alps shows that a microcontinental block known as the Briançonnais terrane existed within this ocean, and was separated from the European plate in the north by the Valais oceanic branch (Frisch, 1979; Handy et al., 2010). Sardinia–Corsica, which has been an internally rigid block since at least the Early Mesozoic (Vigliotti et al., 1990), has a comparable tectonostratigraphy to the Briançonnais continental terrane. These blocks are generally seen as contiguous until the Eocene, when the Briançonnais terrane became incorporated into the western Alps (Figs. 1B, C) (Stampfli et al., 2002; Schmid et al., 2004; Handy et al., 2010).

Testing whether Sardinia–Corsica–Briançonnais was part of Iberia or not requires knowledge on relative Iberia–Eurasia motions, which are constrained based on the interpretation of marine magnetic anomalies in the Bay of Biscay and the Atlantic Ocean (Savostin et al., 1986; Olivet, 1996; Rosenbaum et al., 2002a; Sibuet et al., 2004; Capitanio and Goes, 2006; Vissers and Meijer, 2012a, 2012b), and the dimension of the Iberian continental landmass in the geological past. Early reconstructions (Savostin et al., 1986; Olivet, 1996) inferred that Iberia moved sinistrally along SW Eurasia, and the Valais Ocean was therefore connected to and of the same age as the Bay of Biscay. Later re-interpretations of marine magnetic anomalies suggested that the Bay of Biscay opened due to a vertical-axis rotation of Iberia relative to Europe around a pole located in the eastern Bay of Biscay sometime during the Cretaceous Normal Superchron (121–83 Ma) (Rosenbaum et al., 2002a; Sibuet et al., 2004; Vissers and Meijer, 2012a, 2012b). This hypothesis, supported by a well-documented Aptian–lower Albian (~121–110 Ma) ~35° ccw rotation of Iberia (Van der Voo, 1969; Gong et al., 2008) and Pangea fits at 200 Ma (Ruiz-Martinez et al., 2012), requires synchronous ~N-S convergence between Iberia and Eurasia east of the Bay of Biscay with magnitude increasing eastwards (e.g., Vissers and Meijer, 2012b).

N-S convergence to the east of the Pyrenees is well-known in the Provençe region (Fig. 1A), but is Eocene in age (Lacombe and Jolivet, 2005; Andreani et al., 2010; Espurt et al., 2012). Balanced cross-sections by these authors show at least some tens of kilometers of shortening between Corsica–Sardinia and rigid Eurasia during that time. Excellent bathymetric fits between the Sardinia–Corsica and Provençe margins show that at the beginning of the Oligocene, Sardinia–Corsica was adjacent to the Provence margin (e.g. Bache et al., 2010).

Since the Oligocene, the African subducting plate started to experience major roll-back, which generated extensional back-arcs in the overriding Eurasian plate including the Liguro-Provençal

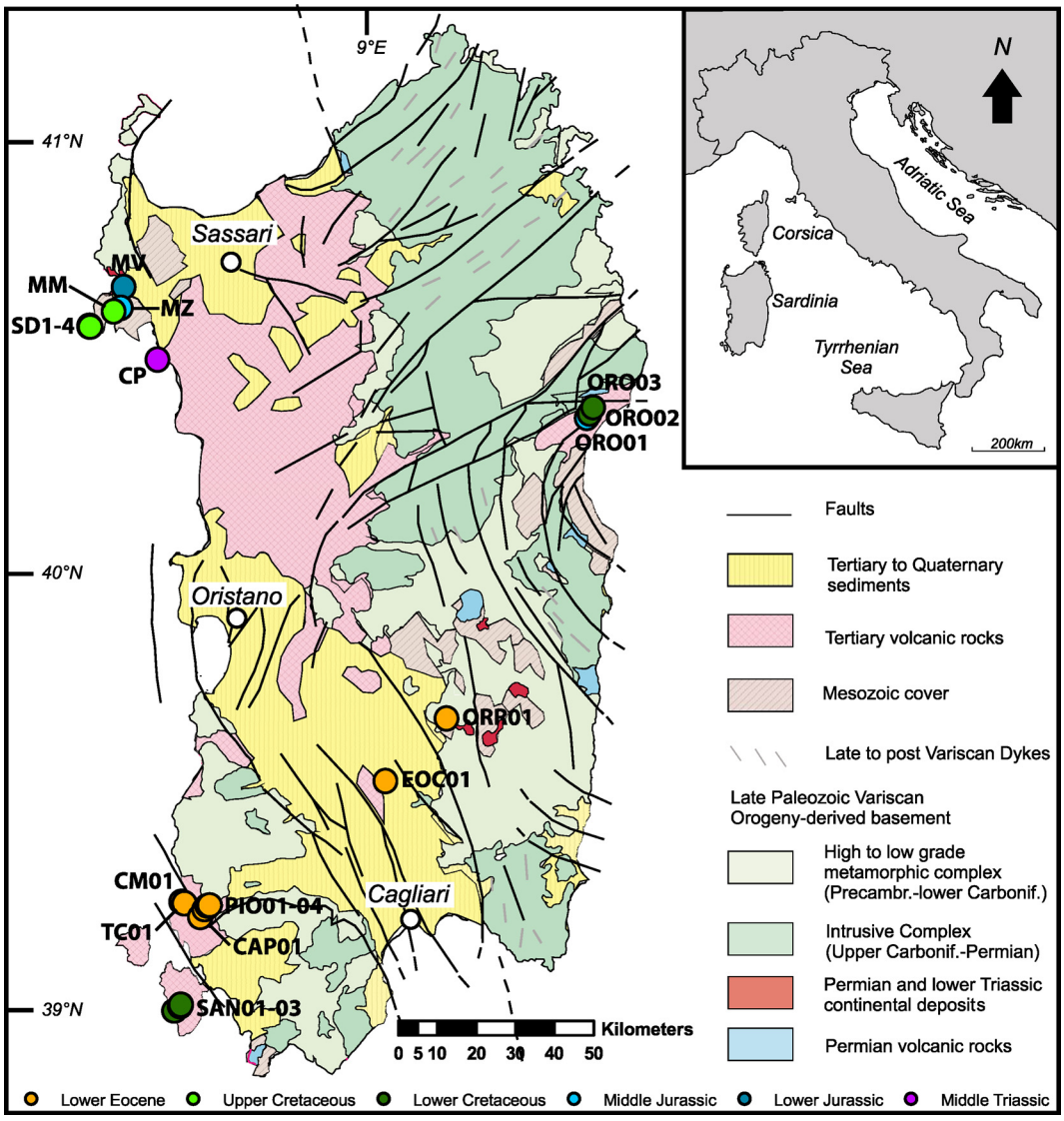


**Fig. 2.** Simplified geological map of Sardinia showing the main lithologies, structures and sampling sites, based on Cherchi et al. (2010), including modifications from Kirscher et al. (2011). Sampling locations are colored according to age.

basin (Malinverno and Ryan, 1986; Rosenbaum et al., 2002b; Faccenna et al., 2004; Jolivet et al., 2009; Handy et al., 2010; van Hinsbergen et al., 2014) (Fig. 1A). The Oligocene opening stage of the Liguro-Provençal Basin, between ~30–21 Ma, was not associated with significant vertical-axis rotation of Sardinia–Corsica (Séranne, 1999). Subsequent oceanization of the Liguro-Provençal Basin between 21 and 16 Ma was, however, accommodated by a ~50° ccw rotation of Sardinia–Corsica relative to Eurasia (Gattacceca et al., 2007). Simultaneous rotations of comparable magnitude also affected the western Alps to the north (Maffione et al., 2008) as well as the most internal domains of the incipient Apenninic chain to the east (Caricchi et al., 2014). Further rollback subsequently induced the opening of the Tyrrhenian Sea to the east of Corsica–Sardinia (Malinverno and Ryan, 1986; Faccenna et al., 2001b; Rosenbaum and Lister, 2004; Cifelli et al., 2007), and major counterclockwise rotations in the Apennines associated to thrust sheets emplacement (Muttoni et al., 2000; Cifelli and Mattei, 2010; Maffione et al., 2013; Caricchi et al., 2014).

## 3. Paleomagnetic sampling, analysis, and results

We sampled the Triassic, Jurassic, Lower and Upper Cretaceous, and Lower Eocene carbonatic units of Sardinia (Fig. 2). Because carbonates are commonly characterized by low ferromagnetic mineral content that may result into unstable and noisy paleomagnetic signal, we collected a large number of samples (~700) from 23 locations to increase the chance of success.

### 3.1. Sampling and laboratory treatment

Paleomagnetic core samples were collected using a gasoline-powered portable drill, and oriented in situ with a magnetic compass corrected for local declination. Magnetic remanence of samples was investigated through thermal and alternating field (AF) demagnetization. AF demagnetization was carried out using an in-house developed robotic 2G Enterprises SQUID magnetometer (noise level $10^{-12}$ A m$^2$), through variable field increments (2–10 mT) up to 70–100 mT. In those samples where high-coercivity, low-blocking temperature minerals (i.e. goethite) were expected, a pre-heating to 150 °C was coupled to AF demagnetization. Stepwise thermal demagnetization was carried out in laboratory built furnaces, through 20–100 °C increments up to 580 °C (or until complete demagnetization). Magnetic remanence was measured after each demagnetization step on a 2G Enterprises SQUID magnetometer. Demagnetization diagrams were plotted as

orthogonal vector diagrams (Zijderveld, 1967) and the characteristic remanent magnetizations (ChRMs) were isolated via principal component analysis (Kirschvink, 1980). Representative Zijderveld diagrams are shown in Fig. 3. Site-mean directions were evaluated using a Fisher statistics (Fisher, 1953) of virtual geomagnetic poles (VGPs) corresponding to the isolated ChRMs. Here, the N-dependent reliability envelope of Deenen et al. (2011) was applied to assess the quality and reliability of the calculated mean ChRM directions. These criteria assess whether (i) the scatter of virtual geomagnetic poles (VGP) can be straightforwardly explained by paleosecular variation (PSV) of the geomagnetic field ($A_{95min} \leq A_{95} \leq A_{95max}$), (ii) an additional source of scatter ($A_{95} > A_{95max}$) is present besides PSV, or (iii) the scatter underrepresents PSV, which may indicate acquisition of the magnetization in a time period too short to fully sample PSV, e.g. due to remagnetization or inappropriate sampling. We applied a fixed 45° cut-off (e.g., Johnson et al., 2008) to the VGP distributions of each site. In few cases (described in detail in Section 3.2) the 45° cut-off rejected more than 50% of the initial data, yielding statistically (but not geologically) meaningful mean values that have not been used for our tectonic reconstructions.

A fold test (McFadden, 1990) for coeval units to determine the timing of their remanence acquisition compared to deformation (i.e. pre-tilting vs. post-tilting) could only be applied to Early Eocene sites, where a bedding variability amongst different sampling localities was observed. The remaining sites (Triassic, Jurassic and Cretaceous) are all characterized by an internally homogeneous bedding attitude, thus excluding the possibility of applying a fold test at the site level being the statistical parameters identical before and after bedding correction. Similarly, no multiple sites of coeval ages were sampled for those time intervals, denying a between-sites fold test.

### 3.2. Paleomagnetic results

#### 3.2.1. Middle Triassic

Middle Triassic (Ladinian (~242–235 Ma)) limestones were sampled in a quarry near Cala Poglina, north-western Sardinia (site CP, Fig. 2). The sampled interval is a lateral equivalent of the Fassinian (lower Ladinian) to Longobardian (upper Ladinian) *Muschelkalk* (Cherchi, 1985). A total of 70 samples were collected from a 40 m-thick interval. This unit consists of massive grey limestone and dolomitic limestone, and reddish cellular dolomites. Approximately 40% of samples were AF demagnetized, the remaining samples thermally. The results of this site yield a spherical and low dispersion VGP distribution. The statistical properties do not pass the Deenen et al. (2011) criteria: the $A_{95}$ is lower than $A_{95min}$ (Table 1). This suggests either averaging of PSV within each specimen owing to low sedimentation rates, or remagnetization. The tilt corrected mean ChRM direction at this site ($D \pm \Delta D = 296.5° \pm 2.6°$ and $I \pm \Delta I = 38.4° \pm 3.4°$; Table 1) has a westerly orientation suggesting strong ccw rotation relative to Eurasia.

#### 3.2.2. Middle Jurassic

A total of 34 samples was collected from a 41 m-thick Aalenian carbonatic sequence (Cherchi, 1985; Cherchi et al., 2010) at Monte Zirra (site MZ), northwestern Sardinia (Fig. 2). Three sub-sites (MZ1, MZ2 and MZ3) were sampled from basal, middle, and top part of the sequence, respectively. The section consists of oolitic grainstones with layers of detrital sandstone, oosparitic limestones, and oncolitic limestones with crossbeds. The average in-situ ChRM direction calculated from this site gives a $D \pm \Delta D = 355.1° \pm 7.3°$ and $I \pm \Delta I = 59.5° \pm 5.0°$; Table 1) is within error of the present-day field at the sampling locality (000°/59.8°) and suggests a recent remagnetization of these rocks.

Bajocian–Bathonian limestones were sampled (46 cores) at Monte Vaccargiu (site MV) (Fig. 2) (Cherchi, 1985). Almost half of the samples ($N = 22$) were demagnetized with AF treatment; the remaining samples were pre-heated to 150 °C before AF demagnetization. The ChRM directions isolated with both techniques are scattered with a non-spherical distribution of the relative VGPs. A fixed 45° cut-off eliminated 11 of the 24 directions, and the resulting A95 does not satisfy the Deenen et al. (2011) criteria, indicating a scatter well beyond that expected from PSV alone.

A 30 m-thick interval within Bathonian–Callovian oolitic–bioclastic packstones–grainstones (Costamagna et al., 2007) was sampled (27 cores) at the Dorgali quarry near the town of Orosei (site ORO-01; Fig. 2). AF demagnetization gave interpretable results with ChRM components isolated between 30 and 70 mT (Fig. 3). The distribution of the ChRMs is spherical and passes the Deenen et al. (2011) criteria (Table 1). Declinations are strongly ccw deviated relative to Eurasia.

#### 3.2.3. Lower Cretaceous

Berriasian–Valanginian (Chabrier et al., 1975) limestones were sampled at three localities (SAN-01, SAN-02, SAN-03) near Sant'Antioco, southwest Sardinia (Fig. 2). The low NRM intensities (0.02–1.2 mA/m) characterizing these sites are probably responsible for the very high scatter of the ChRMs/VGPs, although sites SAN-01 and SAN-03 may represent PSV (Table 1).

Berriasian and Barremian carbonatic sequences (Dieni and Massari, 1963a, 1965; Wiedmann and Dieni, 1968) were sampled in sites ORO-02 and ORO-03 near the town of Orosei (Fig. 2). Very low NRM intensities characterize these rocks (<0.01 mA/m) yielding noisy demagnetization diagrams (Fig. 3). The isolated ChRMs are highly scattered, although they may, after a fixed 45° cutoff, be explained by PSV.

Limestones of Valanginian (SD-1) and Hauterivian–early Barremian (SD-2) age were sampled at the locality of Cala Dragonara (Cherchi, 1985), northern Sardinia (Fig. 2). Both sites are characterized by very low NRM intensities (<0.1 mA/m). Site SD-1 shows completely scattered ChRM directions, and a fixed 45° cut-off eliminates 22 out of 30 obtained directions, yielding no geologically meaningful result. Similarly, site SD-2 displays a scatted that is beyond that expected from PSV alone (Table 1).

#### 3.2.4. Upper Cretaceous

Upper Cretaceous (Coniancian–Santonian) reef bioclastic limestones rich in rudists and corals (Cherchi, 1985) were sampled at Cala Dragonara (SD-3, 33 samples) and Monte Murrone (MM, 118 samples), northwestern Sardinia (Fig. 2). Approximately half of the samples were demagnetized thermally, the other half using AF demagnetization. Thermal demagnetization yielded more stable demagnetization diagrams (Fig. 3). The VGP scatter for site SD-3 can be straightforwardly explained by PSV alone, whereas site MM has a scatter somewhat higher than expected from PSV ($A_{95} > A_{95max}$; Table 1).

Finally, a total of 37 cores were collected at site SD-4 from the uppermost part of the Santonian section of Cala Dragonara (Fig. 2) (Cherchi, 1985; Simone and Cherchi, 2009). ChRMs directions isolated with both AF and thermal treatment show a significant scatter somewhat higher than expected from PSV ($A_{95} > A_{95max}$; Table 1).

#### 3.2.5. Lower Eocene

In south-western Sardinia we have sampled limestones of "Miliolitico" *Auct.*, of early Ypresian age (~56–48 Ma) (Murru and Salvadori, 1990; Raponi, 2003; Cherchi et al., 2008). In central Sardinia coeval limestones with alveolinids and miliolids were sampled. Samples were collected from in total eight sites

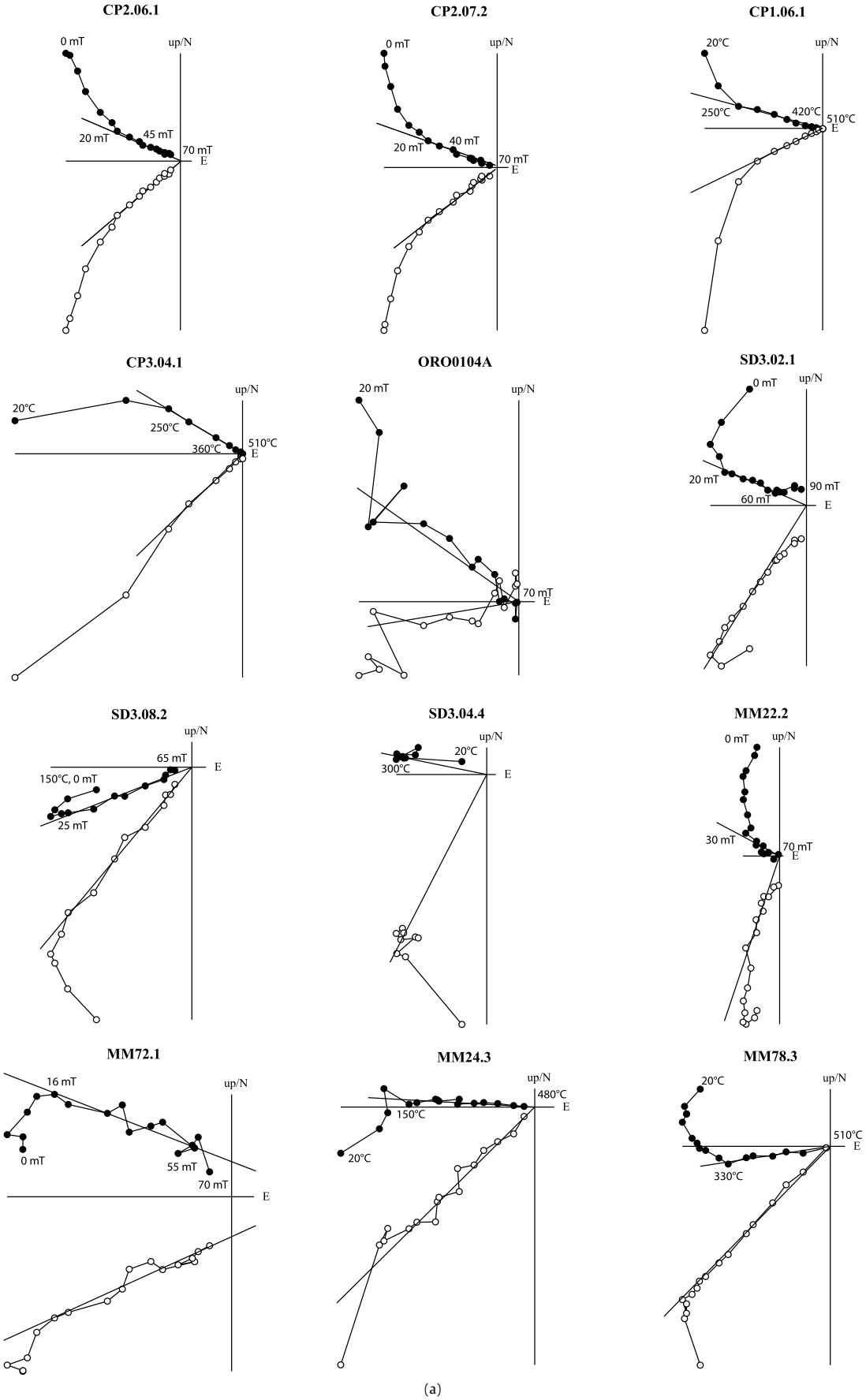


(a)

**Fig. 3.** Orthogonal vector diagrams (Zijderveld, 1967) for representative specimens. Solid and open dots represent projection on the horizontal and vertical planes, respectively. Demagnetization step values are in mT or/and in °C. All vectors are shown after bedding tilt correction.

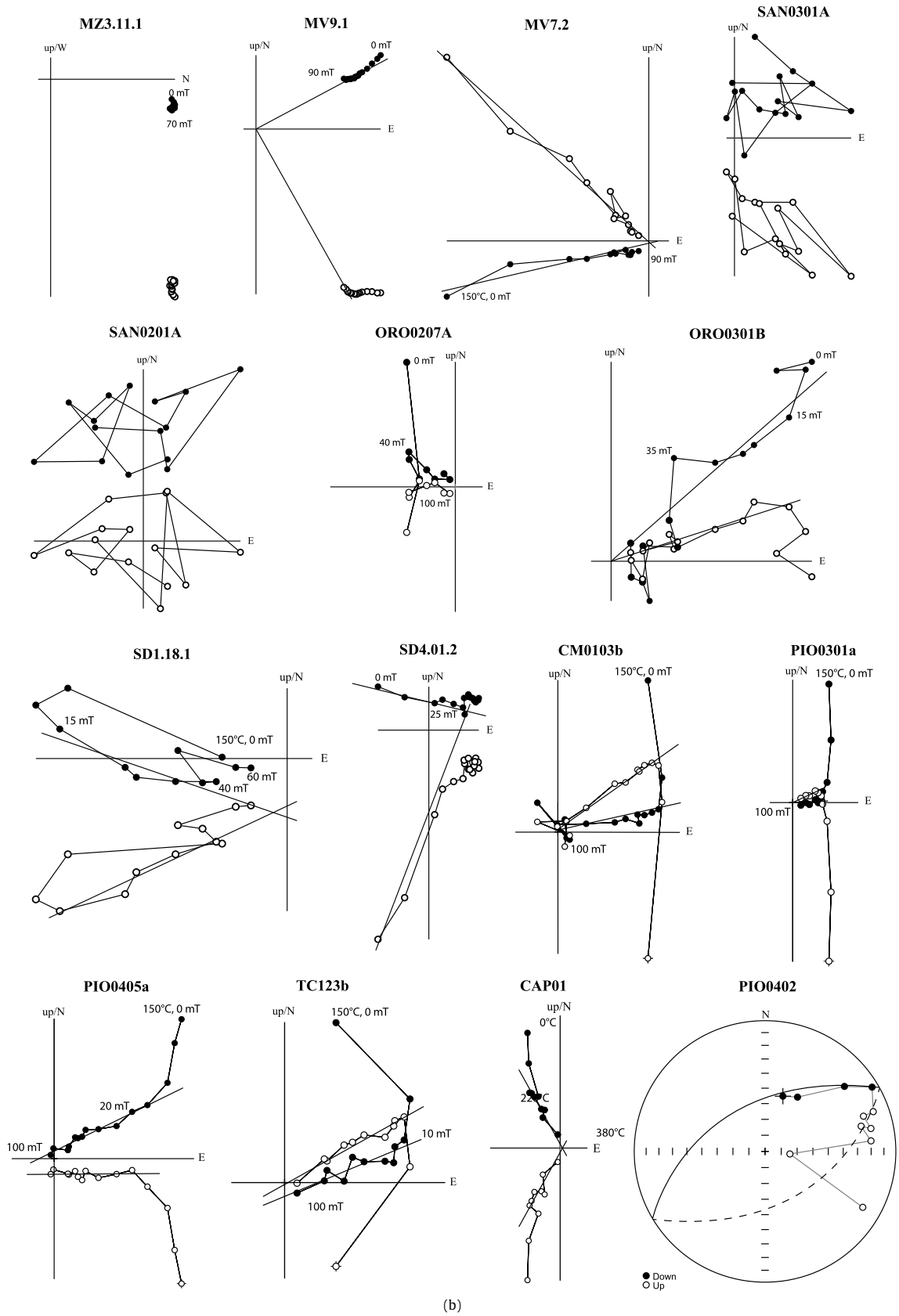


(b)

**Fig. 3.** (continued)

**Table 1**
Statistical parameters per sampled site corrected for bedding tilt (except site MZ, see text). $A_{95}$ = 95% cone of confidence on VGP's; $A_{95min/max}$ = confidence envelope for $A_{95}$ values of Deenen et al. (2011); $\alpha_{95}$ = 95% cone of confidence assuming Fisherian distribution of paleomagnetic directions (not recommended, see (Butler, 1992; Deenen et al., 2011); ΔAge = age uncertainty, using the timescale of Gradstein et al. (2012); $D$ = declination; $\Delta D$ = 95% confidence interval in declination following Butler (1992); $I$ = inclination; $\Delta I$ = 95% confidence interval in inclination following (Butler, 1992); $K$ = precision parameter of Fisher (1953) for VGP distribution; $k$ = precision parameter of Fisher (1953) for average direction assuming Fisherian distribution of paleomagnetic directions (not recommended, see Butler, 1992; Deenen et al., 2011); lat = latitude; lon = Longitude; $N$ = number of interpreted ChRM directions/VGP's; $N_{45}$ = number of directions/VGP's that pass a fixed 45° cutoff. Sites marked by ∗ recorded a present-day field overprint.

| Stratigraphic level | Code | lat | lon | Age | Age | ΔAge | $N$ | $N_{45}$ | Tilt corrected parameters | | | | | | | | | | Bedding | In-situ | |
|---|---|---|---|---|---|---|---|---|---|---|---|---|---|---|---|---|---|---|---|---|---|
| | | | | | | | | | $D$ | $AD$ | $I$ | $\Delta I$ | $A_{95}$ | $A_{95min}$ | $A_{95max}$ | $K$ | ($\alpha_{95}$) | ($k$) | strike/dip | $D$ | $I$ |
| Middle Triassic | CP | 40.4982 | 8.3677 | Ladinian | 238.5 | 3.5 | 70 | 69 | 296.5 | 2.6 | 38.4 | 3.4 | 2.4 | 3.1 | 5.7 | 52.0 | *2.5* | *48.8* | 153/19 | 312.3 | 47.7 |
| Middle Jurassic | MZ* | 40.6658 | 8.2657 | Aalenian | 172.2 | 1.9 | 34 | 32 | 26.5 | 7.3 | 42.9 | 5.0 | 5.6 | 3.0 | 9.2 | 21.7 | *4.6* | *31.6* | 338/29 | 355.1 | 59.5 |
| | MV | 40.6177 | 8.2578 | Bajocian–Bathonian | 168.2 | 2.1 | 24 | 13 | 224.6 | 17.0 | 8.5 | 33.4 | 17.0 | 4.3 | 16.3 | 6.9 | *21.6* | *4.6* | 073/15 | 227.4 | 15.3 |
| | ORO 1 | 40.3651 | 9.6605 | Bathonian–Callovian | 165.9 | 2.4 | 27 | 27 | 246.0 | 5.1 | 37.2 | 6.9 | 4.7 | 3.2 | 10.3 | 35.3 | *5.0* | *32.5* | 327/20 | 244.5 | 17.4 |
| Lower Cretaceous | ORO 2 | 40.3742 | 9.6703 | Berriasian | 142.4 | 2.6 | 8 | 7 | 348.1 | 24.1 | 25.1 | 40.6 | 23.4 | 5.5 | 24.1 | 7.6 | *25.2* | *6.7* | 340/32 | 332.6 | 25.3 |
| | SAN 1 | 38.9994 | 8.4307 | Berriasian–Valanginian | 139.0 | 6.0 | 9 | 8 | 161.9 | 16.6 | −49.3 | 16.3 | 224.6 | 5.2 | 22.1 | 15.9 | *13.4* | *18.1* | 172/41 | 204.6 | −40.3 |
| | SAN 2 | 39.0119 | 8.4470 | Berriasian–Valanginian | 139.0 | 6.0 | 8 | 5 | 251.8 | 32.8 | 32.6 | 48.7 | 31.1 | 6.3 | 29.7 | 7.0 | *36.5* | *5.3* | 264/10 | 245.9 | 30.0 |
| | SAN 3 | 39.0145 | 8.4494 | Berriasian–Valanginian | 139.0 | 6.0 | 6 | 4 | 40.9 | 29.4 | 6.1 | 58.3 | 29.4 | 6.9 | 34.2 | 10.8 | *42.9* | *5.5* | 224/32 | 44.6 | 6.8 |
| | SD 1 | 40.5757 | 8.1615 | Valanginian | 136.4 | 3.4 | 30 | 8 | 218.3 | 15.9 | −1.2 | 31.9 | 15.9 | 5.2 | 22.1 | 13.0 | *22.8* | *6.9* | 046/19 | 218.3 | 1.4 |
| | SD 2 | 40.5734 | 8.1628 | Hauterivian–early Barremian | 130.3 | 2.6 | 26 | 15 | 262.0 | 16.2 | 21.1 | 28.6 | 15.9 | 4.1 | 14.9 | 6.8 | *20.4* | *4.5* | 046/19 | 266.1 | 9.3 |
| | ORO 3 | 40.3873 | 9.6806 | Barremian | 127.7 | 2.7 | 10 | 7 | 145.0 | 16.8 | 22.0 | 29.5 | 16.5 | 5.5 | 24.1 | 14.4 | *25.6* | *6.5* | 330/35 | 159.1 | 20.7 |
| Upper Cretaceous | SD 3 | 40.5724 | 8.1636 | Coniacian–Santonian | 86.7 | 3.1 | 33 | 19 | 262.4 | 10.6 | 52.7 | 9.3 | 8.8 | 3.7 | 12.8 | 15.4 | *9.3* | *14.0* | 064/23 | 284.3 | 41.1 |
| | MM | 40.6093 | 8.2357 | Coniacian–Santonian | 86.7 | 3.1 | 127 | 92 | 276.8 | 5.7 | 48.8 | 5.7 | 4.9 | 2.0 | 4.7 | 9.9 | *4.6* | *11.5* | 182/11 | 278.3 | 59.7 |
| | SD 4 | 40.5720 | 8.1639 | Santonian | 85.0 | 1.3 | 37 | 18 | 280.6 | 13.9 | 23.9 | 23.9 | 13.6 | 3.8 | 13.3 | 7.4 | *17.9* | *4.7* | 339/13 | 278.4 | 12.7 |
| Paleocene–Eocene | PIO-03 | 39.2412 | 8.5281 | upper Paleocene–lower Eocene | 53.5 | 5.7 | 7 | 7 | 84.4 | 1.5 | −24.6 | 2.5 | 1.4 | 5.5 | 24.1 | 1818.9 | *1.5* | *1529.8* | horizontal | 84.4 | −24.6 |
| | PIO-04 | 39.2443 | 8.5327 | upper Paleocene–lower Eocene | 53.5 | 5.7 | 8 | 8 | 95.2 | 5.2 | −44.0 | 6.0 | 4.7 | 5.2 | 22.1 | 141.6 | *4.0* | *190.2* | 012/6 | 95.8 | −38.0 |
| | CM | 39.2519 | 8.4506 | Lower–Middle Eocene | 49.0 | 9.0 | 19 | 19 | 75.7 | 4.4 | −40.1 | 5.6 | 4.1 | 3.7 | 12.8 | 68.6 | *4.2* | *64.2* | 133/14 | 84.4 | −51.3 |
| | TC | 39.2484 | 8.4588 | Lower–Middle Eocene | 49.0 | 9.0 | 15 | 15 | 80.9 | 5.9 | −44.1 | 6.8 | 5.3 | 4.1 | 14.9 | 52.3 | *4.8* | *64.1* | 147/11 | 86.6 | −53.9 |
| | ORR | 39.6751 | 9.2371 | upper Paleocene–lower Eocene | 53.5 | 5.7 | 6 | 4 | 90.1 | 22.1 | −17.0 | 40.9 | 21.9 | 6.8 | 34.2 | 18.6 | *32.9* | *8.8* | 273/7 | 88.0 | −16.5 |
| | CAP* | 39.2173 | 8.5062 | Lower–Middle Eocene | 49.0 | 9.0 | 9 | 7 | 328.3 | 18.5 | 40.4 | 23.3 | 16.9 | 5.5 | 24.1 | 13.6 | *18.6* | *11.5* | 094/8 | 331.7 | 33.7 |
| | PIO-01* | 39.2332 | 8.5194 | Lower–Middle Eocene | 49.0 | 9.0 | 6 | 4 | 2.6 | 31.4 | 63.4 | 17.0 | 21.5 | 6.8 | 34.2 | 19.3 | *15.3* | *37.2* | 274/11 | 1.6 | 74.8 |
| | PIO-02* | 39.2330 | 8.5188 | Lower–Middle Eocene | 49.0 | 9.0 | 7 | 5 | 20.2 | 42.9 | 45.4 | 46.4 | 37.4 | 6.3 | 29.7 | 5.1 | *36.4* | *5.4* | 266/13 | 27.8 | 56.9 |

(TC, PIO-01/02/03/04, CM, CAP, ORR) from different localities distributed within southwest and central Sardinia (Fig. 2). The magnetic remanence intensity in those rocks is always very low (<0.05 mA/m) and generally results in noisy demagnetization diagrams (Fig. 3). In many cases, a secondary component could not be entirely removed during demagnetizations; from such samples we determined remagnetization great circles. We used the approach of McFadden and McElhinny (1988) (Fig. 4) in combining great circles and linear best fits (setpoints).

The scatter of ChRMs at site PIO-02 is too high ($A_{95} > A_{95max}$; Table 1), and likely related to the low intensity of the remanence. The calculated mean direction is not statistically different from the present-day field direction, suggesting a possibly recent magnetic overprint. The remanence directions of the remaining sites are distributed within two distinct clusters. A first cluster (sites CAP and PIO-01) displays northerly directions that, in the case of site PIO-01, is statistically not distinguishable from that of the present field at the sampling locality (hence likely remagnetized). The remanence directions of site CAP show both normal polarity and an intermediate mean direction between the present field and those of the second cluster. This site has likely been affected by recent partial remagnetization, its mean direction does therefore probably not reflect the Eocene field, and data from this site are not used for further discussion. The second cluster, is formed by five sites (CM, PIO-03, PIO-04, TC, ORR) and is characterized by reverse polarity remanences with easterly directions indicating strong ccw rotations (after transposing the ChRMs to a normal polarity state). The in situ directions of those sites are substantially different from that of the local present field (Table 1). This evidence, together with the positive result of the fold test ($N = 49$; critical $Scos_{95\%} = 8.14$; in situ statistics: Dec = 088.6°/−47.2°, $k = 41.7$, $\alpha_{95} = 3.2°$, $Scos_1 = 28.3$; unfolded statistics: Dec = 082.9°/−41.1°, $k = 57.3$, $\alpha_{95} = 2.7°$, $Scos_1 = 7.2$; maximum $k$ at 98% unfolding McFadden, 1990) indicates a pre-tilt and likely primary acquisition of the magnetization.

## 4. Discussion

### 4.1. Statistical analyses and reconstructing the rotation of Sardinia

Reliable paleomagnetic poles are commonly obtained from sets of paleomagnetic directions showing a scatter that is exclusively induced by paleosecular variation of the magnetic field. PSV leads to a variation in the distribution of the virtual geomagnetic poles of several tens of degrees, but geologically has rather short timescales (e.g., Tauxe et al., 2010). Averaging of PSV therefore requires obtaining a sufficiently large number of individual spot readings over a sufficiently long time interval, but short enough to avoid the effect of plate motion or (local) tectonic rotations. For tectonic purposes, paleomagnetic sampling is commonly carried out at multiple sites to be able to recognize local rotations. The scatter of paleomagnetic directions at individual sampling sites will then reveal if PSV is sufficiently represented. When the scatter of the obtained ChRMs at a site is much larger than can be expected from PSV, or the distribution of the VGP scatter is not approximately circular, the corresponding paleomagnetic pole must be handled with care for tectonic interpretation (Deenen et al., 2011).

It is still common practice in paleomagnetism to average site means, instead of averaging all individual directions of all sites, which better allows assessing whether the sampled scatter is consistent with PSV. This has several disadvantages. Sites with unequal numbers of samples, and hence unequal degrees of averaging of PSV, are given equal importance; the (unequal) statistics of each site mean are not taken into account. Hence, the statistical properties of the average of site means bears no information on the ChRM and VGP distributions, and do not allow comparison with the expected PSV (Deenen et al., 2011). Indeed, many of our (and published) sites have $A_{95}$ values that exceed the Deenen et al. (2011) confidence envelope. Discarding those sites, however, may discard valuable information.

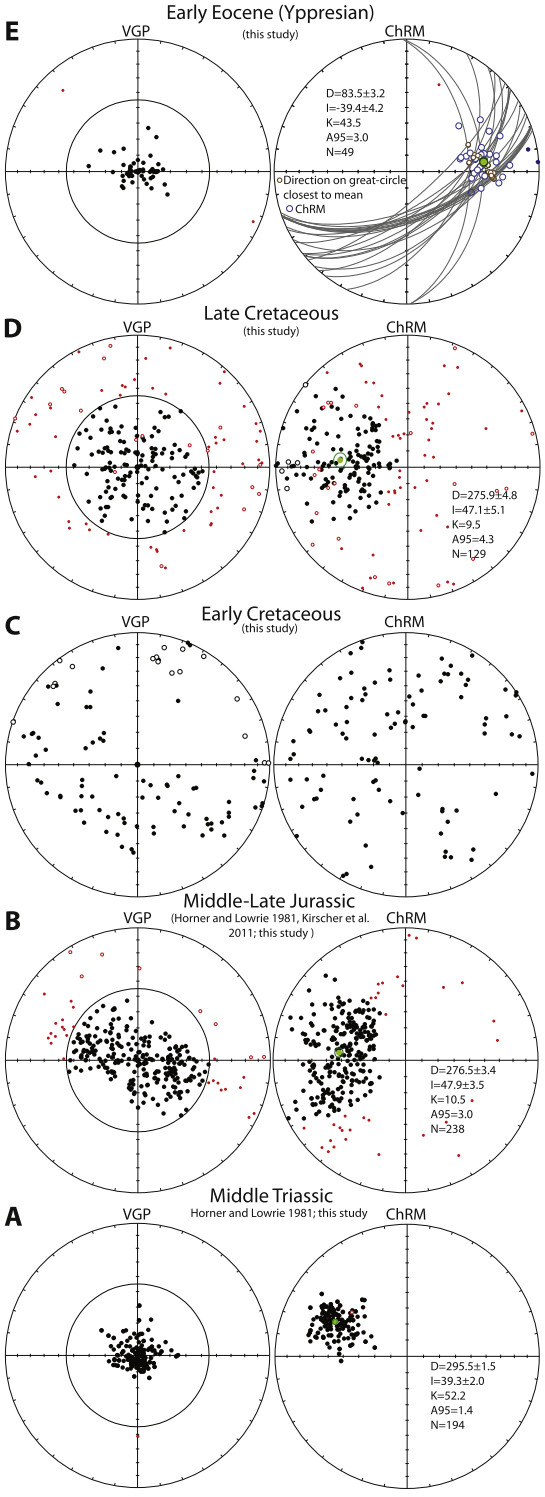


**Fig. 4.** Equal area projections with all paleomagnetic data, averages, and statistical properties from Sardinia from the A) Middle Triassic; B) Middle–Upper Jurassic (all converted to normal directions); C) Lower Cretaceous; D) Upper Cretaceous and E) Lower Eocene (with ChRMs interpreted directly from orthogonal vector plots as blue circles, and ChRMs interpreted from remagnetization great circles in brown circles). VGP plots on the left are centered around the mean VGP. (For interpretation of the references to color in this figure legend, the reader is referred to the web version of this article.)

**Table 2**
Average directions computed per stratigraphic interval, and corresponding statistical parameters. For abbreviations, see caption of Table 1.

| Code | Age | Remark | Age | ΔAge | $N$ | $N_{45}$ | $D$ | $\Delta D$ | $I$ | $\Delta I$ | $A_{95}$ | $A_{95min}$ | $A_{95max}$ | $K$ |
|---|---|---|---|---|---|---|---|---|---|---|---|---|---|---|
| A | Triassic | this study; Horner and Lowrie, 1981 | 236.9 | 8.1 | 196 | 194 | 295.5 | 1.5 | 39.3 | 2.0 | 1.4 | 1.5 | 3.0 | 52.2 |
| B | Middle–Late Jurassic | this study; Horner and Lowrie, 1981; Kirscher et al., 2011 | 160.0 | 15.0 | 270 | 238 | 276.5 | 3.4 | 47.9 | 3.5 | 3.0 | 1.3 | 2.6 | 10.2 |
| C | Early Cretaceous | this study | 135.0 | 10.0 | *no meaningful result* | | | | | | | | | |
| D | Late Cretaceous | this study | 86.8 | 3.0 | 197 | 129 | 275.9 | 4.8 | 47.1 | 5.1 | 4.3 | 1.7 | 3.8 | 9.5 |
| E | Paleocene–Eocene | this study | 49.6 | 9.6 | 55 | 49 | 83.5 | 3.2 | −39.4 | 4.2 | 3.0 | 2.5 | 6.7 | 43.5 |

Therefore, we follow a different approach, and combine all measured and published individual paleomagnetic directions of specific time intervals sampled in Sardinia, except the Miocene averages, which we adopt from Gattacceca et al. (2007). We subsequently discuss the data distribution for each period in terms of its shape and statistical properties, to assess whether it is related to PSV, remagnetization, or between-site local rotations.

To be able to compare our new data to published results, we have digitized the paleomagnetic directions obtained from Middle Triassic and Upper Jurassic rocks from equal area projections published by Horner and Lowrie (1981). Middle and Upper Jurassic rocks were paleomagnetically studied by Kirscher et al. (2011), but these authors only give site averages (with amounts of samples varying from one to thirteen per site). To weigh these site averages equally, we performed a parametric (Fisherian) sampling of each of their sites, using their published number of samples ($N$) and dispersion parameter ($k$) per site. We have subsequently plotted and averaged all digitized or parametrically sampled data together with our new results in five age bins: Middle Triassic, Middle–Late Jurassic, Early Cretaceous, Late Cretaceous and Early Eocene (Fig. 4; Table 2).

Results from the Middle Triassic of our study (site CP) and reported by Horner and Lowrie (1981) provide an average direction $D \pm \Delta D = 295 \pm 1.5°$, $I \pm \Delta I = 39.3 \pm 2.0$. This declination would suggest a rotation of ∼90° ccw relative to the expected declination for Eurasia based on the Global Apparent Polar Wander Path (APWP) of Torsvik et al. (2012) (Fig. 7). This seems consistent with the results of Jurassic and younger rocks from Sardinia (see below), but nevertheless some doubt exists whether the obtained direction is representing the Middle Triassic paleomagnetic field. Firstly, the distribution of the data is tightly clustered, more than can be expected from PSV (i.e., $A_{95} < A_{95min}$, Table 2). This may point to a (rapid) remagnetization. Secondly, the paleolatitude derived from the inclination is ∼15° more northerly than predicted by the APWP of Eurasia (Fig. 5B; Table 2). Lower inclinations than expected can be explained by inclination shallowing caused by compaction (Tauxe, 2005), but steeper inclinations are difficult to explain. It is interesting to note that the latitude recovered from the Triassic rocks would be consistent with the expected paleolatitude for Eurasia in the 170–140 Ma time interval, which coincides with the opening of the Piemonte-Ligurian Ocean of which Sardinia formed a margin (Vissers et al., 2013). Extensional deformation and associated fluid flow may have remagnetized the Triassic rocks, in a similar way as recorded, for example, in pervasive syn-extensional northern Iberian remagnetizations (Gong et al., 2009). Although the mean declination for the Triassic sites may represent a later (Jurassic) remagnetization, it indicates post-Triassic (or Jurassic) major ccw rotation of Sardinia–Corsica.

The average from Middle to Upper Jurassic rocks obtained by Horner and Lowrie (1981), Kirscher et al. (2011), and in this study (site ORO-01) gives, after converting all directions to normal polarity, $D \pm \Delta D = 276.5 \pm 3.4°$, $I \pm \Delta I = 47.9 \pm 3.5°$ (Fig. 4, Table 2). The inferred paleolatitude is within error with that predicted by the European APWP (Fig. 5B), and the mean declination documents a ccw rotation of ∼95° of Sardinia relative to Europe (Fig. 5A). A close inspection of the VGP distribution (Fig. 4), however, shows an elongated pattern. VGP distributions that represent PSV would have a circular distribution, and hence the distribution of the Jurassic data suggests an additional source of scatter. This is further confirmed by the $A_{95}$, which is somewhat higher than $A_{95max}$ (Table 2). We suggest that this additional source of scatter is related to some local (low-magnitude) rotations of one site relative to another (the Jurassic data come from approximately 20 different sites), possibly as a result of e.g., Middle Eocene transpressional deformation that affected Sardinia (Trémolières et al., 1984; Carosi et al., 2005; Buttau et al., 2008; Cherchi et al., 2008; Barca and Costamagna, 2010). The consistency between the obtained average for the Jurassic, and the Cretaceous and Eocene averages (see below), however, leads us to believe that these local rotations are likely averaged out within this very large dataset ($N = 238$; Fig. 4).

The results from the Lower Cretaceous units obtained in this study (seven sites; Table 1) do not yield a meaningful paleomagnetic pole because of the random pattern of the observed directions (Fig. 4). This is probably caused by the very low intensity of the remanence, which is commonly close to the noise level of the magnetometer. Conversely, the results from the Upper Cretaceous rocks (three sites; Table 1) are scattered but consistent, and yield an average direction of $D \pm \Delta D = 275.9 \pm 4.8°$, $I \pm \Delta I = 47.1 \pm 5.1°$. The paleolatitude calculated from the obtained inclination is within error of that predicted by the APWP (Torsvik et al., 2012) (Fig. 5B). Comparison of the declination with the APWP shows a ccw rotation of ∼90° of Sardinia relative to the Europe. Although the scatter of Late Cretaceous directions is somewhat larger than expected from PSV alone ($A_{95} > A_{95max}$, Table 2), the distribution of VGPs is near-circular (Fig. 4) suggesting that the additional source of scatter is random. We explain this excess scatter to result from uncertainties in the determination of the ChRMs owing to the low magnetic intensities of the samples, so we consider the obtained average to reliably represent the Late Cretaceous magnetic field.

Finally, most specimens from sites of the Lower Eocene show an unresolved present-day (normal polarity) overprint that often affects the original reversed polarity directions. Many demagnetization results were therefore interpreted using remagnetization great circle analysis (Fig. 4) following the approach of McFadden and McElhinny (1988). The combination of setpoints and great circles provided a consistent mean direction of $D \pm \Delta D = 083.5 \pm 3.2°$, $I \pm \Delta I = -39.4 \pm 4.2°$. The statistical values of this dataset pass the Deenen et al. (2011) criteria. The mean paleomagnetic direction obtained from the Lower Eocene units documents a ∼100° ccw rotation of Sardinia relative to Eurasia. The inclination (and thus the paleolatitude) is a few degrees lower than the reference direction, which could well have been caused by inclination shallowing.

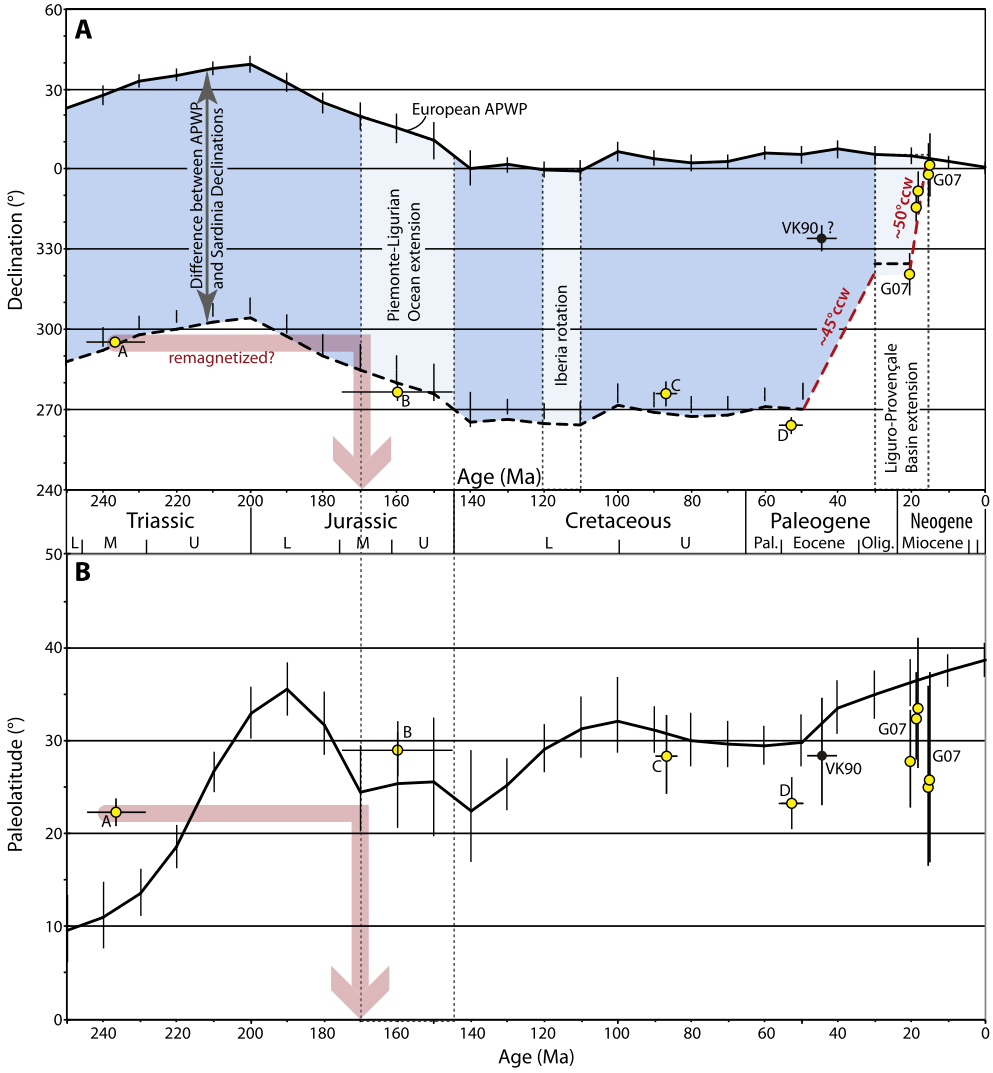


**Fig. 5.** (A) Declination versus age plot of paleomagnetic sites from Sardinia, and the Global Apparent Polar Wander Path (APWP) of Torsvik et al. (2012) for stable Eurasia in Sardinian coordinates. The colored envelope represents the difference between the APWP for Eurasia and the expected declinations for Sardinia (a 95° ccw translated curve until the Eocene). Two rotational phases inferred in this paper are shown: a ~45° ccw *rotation phase 1* between ~55 Ma and the onset of extension in the Liguro-Provençal Basin (~30 Ma Séranne, 1999), and a ~50° ccw *rotation phase 2* between 21 and 16 Ma following Gattacceca et al. (2007). (B) Paleolatitude versus age. Note the higher than expected paleolatitude for the Triassic, inferred to be remagnetized in the Jurassic. A–D refer to data entries in Table 2. VK90 = Vigliotti and Kent (1990), G07 = Gattacceca et al. (2007). Datapoints A, B and C include data from Horner and Lowrie (1981) and Kirscher et al. (2011). (For interpretation of the references to color in this figure legend, the reader is referred to the web version of this article.)

### 4.2. Paleogeography of the Mediterranean region

The main aim of this study is to test whether the pre-Oligocene ccw rotation of Sardinia, previously documented by studies of Horner and Lowrie (1981) and Kirscher et al. (2011), occurred synchronously with the Early Cretaceous rotation of Iberia (Gong et al., 2008). Our results unequivocally demonstrate that Sardinia did not experience major rotations between Jurassic and Early Eocene times, but underwent a ~95° ccw rotation in Eocene and younger times (Fig. 5A). This has major implications for the palaeogeographic reconstruction of the western Mediterranean during Mesozoic–Cenozoic times. On the basis of our new results, we must conclude that the SCB block has been separated by a plate boundary from Iberia in Cretaceous times. In left-lateral transtensional opening models of the Bay of Biscay (Olivet, 1996; Savostin et al., 1986), such a plate boundary should have been E-W convergent. There is little evidence, however, for extensive Mesozoic E-W shortening in eastern Iberia or southern Sardinia (where it should be N-S shortening in present-day coordinates). Rotational opening models for the Bay of Biscay, with a pivot in the eastern Bay of Biscay (Rosenbaum et al., 2002a; Sibuet et al., 2004; Vissers and Meijer, 2012a, 2012b), require a pre-Oligocene dextral transform plate boundary between Iberia and Sardinia. Such a transform may well have existed, and may have been re-used to form the modern North Balearic Transform Zone (Fig. 1) (Séranne, 1999; van Hinsbergen et al., 2014). Our proposed reconstruction for the Mediterranean region (Fig. 6) therefore follows the Bay of Biscay-Central Atlantic model of (Vissers and Meijer, 2012a, 2012b), embedded in the Atlantic plate circuit based on Gaina et al. (2002) and Müller et al. (1999).

The restoration of the Liguro-Provençal back-arc basin back-rotates Sardinia–Corsica by ~50° around an Euler pole located north of Corsica, yielding an accurate fit between the bathymetric contours of Provence and the western Sardinia–Corsica margin around 30 Ma, when extension in this basin started (Bache et al., 2010, and references therein). The Eocene rotation of Sardinia documented in this study could not have occurred around the same Euler pole, as that would generate a complete overlap between Sardinia and the Provençe. Since the Eocene N-S shortening documented in Provence (Lacombe and Jolivet, 2005;

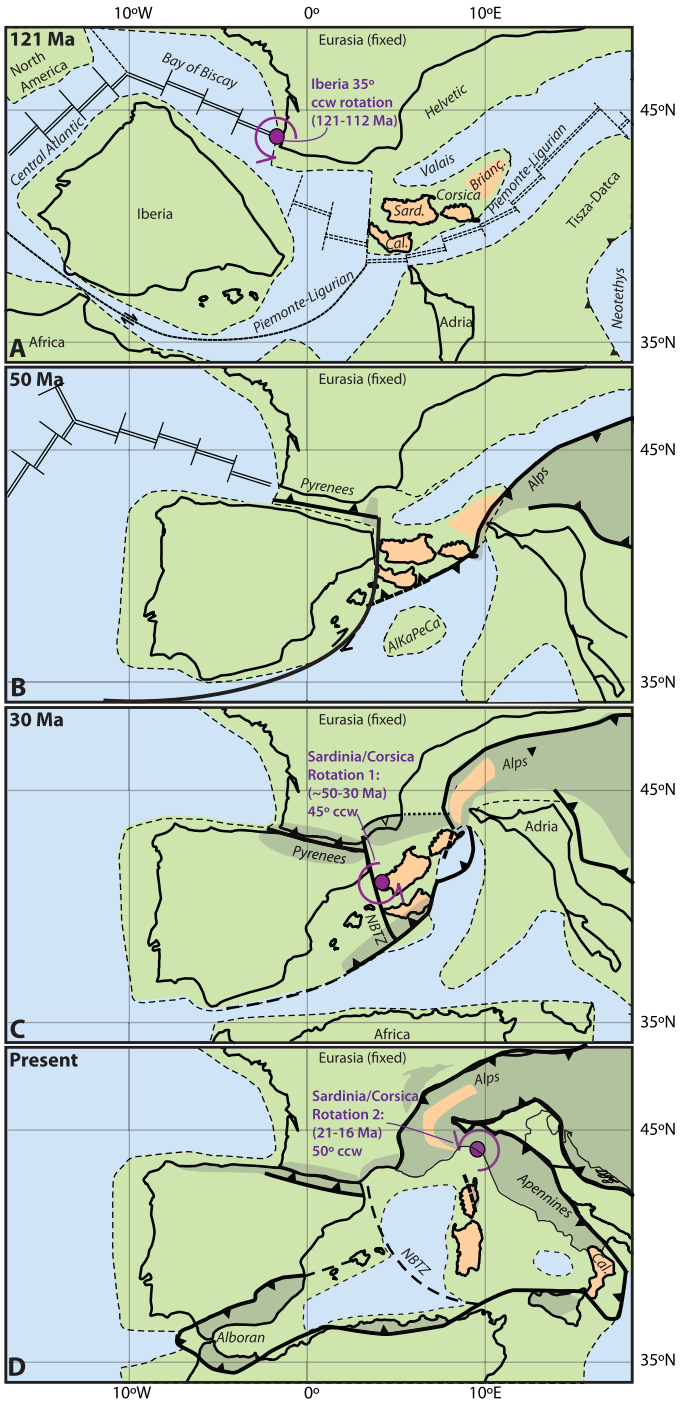


**Fig. 6.** Tectonic reconstructions of the central-western Mediterranean based on the results of this study. (A) 121 Ma, i.e. preceding the rotation of Iberia; (B) 50 Ma, at the inferred onset of the Eocene Corsica–Sardinia rotation; (C) 30 Ma, at the onset of opening of the Liguro-Provençal Basin; (D) present-day. Eurasia–North America–Iberia–Africa plate circuit follows Torsvik et al. (2012), Gaina et al. (2013) and Vissers and Meijer (2012a, 2012b), in a Mercator projection. Reconstruction of the SW Mediterranean subduction zones since Eocene time follows van Hinsbergen et al. (2014). Dimension of the Piemonte-Ligurian Ocean adopted from Vissers et al. (2013). Euler poles for Corsica–Sardinia rotations versus Europe given in Table 3 were estimated using GPlates reconstruction software (www.gplates.org, Boyden et al., 2011). Abbreviations: AlKaPeCa (Al = Alboran, southern Spain and northern Morocco, Ka = Kabylides, Algeria, PeCa = Calabria–Peloritai Arc). NBTZ = North Balearic Transform Zone. Poles of Iberia and Sardinia–Corsica rotations are the purple dots with arrow.

**Table 3**
Estimated finite Euler rotations for Corsica–Sardinia versus Europe. Timing and amount of Miocene rotations come from Gattacceca et al. (2007); reconstruction of the Liguro-Provençal basin based on Séranne (1999); Eocene rotation based on this study. Euler poles are estimated using *GPlates* plate reconstruction software (www.gplates.org; Boyden et al., 2011).

| Finite Euler poles for Corsica–Sardinia versus Eurasia | | | |
|---|---|---|---|
| Age | Latitude | Longitude | Rotation |
| 0.0 | 0.0 | 0.0 | 0.0 |
| 16.0 | 0.0 | 0.0 | 0.0 |
| 21.5 | −42.5 | −170.5 | 50.0 |
| 30.0 | −43.7 | −170.6 | 50.0 |
| 50.0 | −41.8 | −172.2 | 5.0 |

Andreani et al., 2010; Espurt et al., 2012) is coeval with the Eocene ~45° ccw rotation phase for Sardinia documented in this study, we argue that these two processes have a causal relation. A kinematic scenario accommodating this rotation with the minimum amount of shortening, and involving no extension, places the Euler pole on the SW corner of Sardinia (Fig. 6). This scenario predicts up to ~100 km of Sardinia–Eurasia convergence at the longitude of the eastern Provence, i.e. higher than the several tens of km documented onshore (Espurt et al., 2012). The remaining convergence was likely accommodated in the now-stretched passive margins of the Liguro-Provençal basin.

Our paleomagnetic data show that the Eocene rotation occurred coeval with the onset of incorporation of the Briançonnais continental domain, which was likely attached to Corsica, into the Alps since 55 Ma, when it came into collision with the northern margin of Adria (Handy et al., 2010). West of Adria, however, oceanic subduction continued with a southward, 'Alpine' subduction polarity on Corsica, but likely with a northward polarity below Sardinia, as documented in the nappe stack of Calabria (e.g., Faccenna et al., 2001a; Rossetti et al., 2004; Heymes et al., 2010; van Hinsbergen et al., 2014). We interpret the Eocene rotation of Sardinia–Corsica as the result of the interplay between these two subduction systems, whereby the southward subduction zone of the Alps retreated northward relative to a more stationary northward subduction zone from southwest Sardinia westwards. As a result, the intervening Sardinia–Corsica segment rotated counterclockwise, and the subduction zones below these became increasingly more oblique, consistent with Eocene transpressive deformation documented from several localities of Sardinia (Carosi et al., 2005; Buttau et al., 2008). Our reconstruction assumes a ~45° ccw Eocene rotation of Sardinia–Corsica around an Euler pole in southernmost Sardinia (in modern coordinates). Rotation started simultaneously with the incorporation of the Briançonnais terrane into the Alps, i.e. ~55 Ma, and continued until the onset of opening of the Liguro-Provençal basin, i.e. ~30 Ma (Table 3). This requires a maximum Corsica–Europe convergence of ~300 km, which is equal to the contemporaneous Africa–Europe convergence constrained by Atlantic ocean reconstructions (Müller et al., 1999; Gaina et al., 2002). One paleomagnetic result from Corsica, from Lutetian (~49–40 Ma) sediments by Vigliotti and Kent (1990) gave ~35° ccw rotation. If this result represents the Lutetian paleomagnetic field, it would yield an early Eocene rotation rate of Corsica–Sardinia that is much faster than can be explained by Africa–Europe convergence. This would require major N-S extension between Corsica and Africa, for which there is no geological evidence. In addition, the Eocene result of Vigliotti and Kent (1990) would represent an unlikely smaller rotation than that derived from younger (lower Miocene) volcanics studied by Gattacceca et al. (2007). This could imply that their Eocene site has been remagnetized in the Miocene, similar to other Eocene sediments from Corsica reported in the same study.

Our study shows that major block rotations may occur at the transition region between oppositely dipping subduction zones. A similar mechanism may have been responsible for the bending of the southwestern Alpine arc synchronous with the Miocene Sardinia–Corsica rotation, as proposed by Maffione et al. (2008). The increasing obliquity of the Eocene subduction zones of Corsica may have aided the late Eocene reversal of subduction polarity below Corsica (Fig. 6), as suggested by Argnani (2012).

## 5. Conclusions

In this paper, we provide new paleomagnetic results from Triassic, Jurassic, Lower and Upper Cretaceous and Lower Eocene carbonate rocks from Sardinia, and integrate them with existing data from Triassic and Jurassic units throughout Sardinia. From all stratigraphic intervals, a declination was recovered that deviates ∼95° ccw relative to Eurasian reference directions. This demonstrates that Sardinia did not follow the well-documented ∼35° counterclockwise rotation of Iberia in the Aptian, implying that the Sardinia–Corsica block must have been separated from Iberia by a (transform) plate boundary at that time. Published Lower Miocene volcanics from Sardinia recorded a ∼50° ccw rotation genetically related to the opening of the Liguro-Provençal back-arc basin. Our results demonstrate that the Sardinia–Corsica block experienced ∼45° ccw rotation in the Eocene, prior to the onset of extension in the Liguro-Provençal Basin around 30 Ma. We argue that this Eocene rotation of Sardinia–Corsica is synchronous with documented N-S shortening in the Provence and that it occurred simultaneously with the incorporation of the Briançonnais continental domain in the Alps after Adria collision. We explain this rotation as a result from the interplay between a southward 'Alpine' subduction zone at Corsica, retreating northward, and a northward subduction zone below Sardinia, remaining relatively stationary versus Eurasia.

## Acknowledgements

We thank Mark Dekkers and Maud Meijers for discussion. Rinus Wortel is thanked for help during sampling. This work was supported by the ISES Central Field Studies fund of the Netherlands Research School for Integrated Solid Earth Sciences (ISES). D.J.J.v.H. and M.M. acknowledge funding through ERC Starting Grant 306810 (SINK) and NWO VIDI grant 864.11.004 to D.J.J.v.H. We are grateful for the constructive comments by Yanick Ricard (editor), Jérôme Gattacceca, Fabio Speranza and an anonymous reviewer.

## References

Andreani, L., Loget, N., Rangin, C., Le Pichon, X., 2010. New structural constraints on the southern Provence thrust belt (France): evidences for an Eocene shortening event linked to the Corsica–Sardinia subduction. Bull. Soc. Géol. Fr. 181, 547–563.

Argnani, A., 2012. Plate motion and the evolution of Alpine Corsica and Northern Apennines. Tectonophysics 579, 207–219. http://dx.doi.org/10.1016/j.tecto.2012.06.010.

Bache, F., Olivet, J.-L., Gorini, C., Aslanian, D., Labails, C., Rabineau, M., 2010. Earth Planet. Sci. Lett. 292, 345–356.

Barca, S., Costamagna, L.G., 2010. C. R. Géosci. 342, 116–125.

Boyden, J.A., Müller, R.D., Gurnis, M., Torsvik, T.H., Clark, J.A., Turner, M., Ivey-Law, H., Watson, R.J., Cannon, J.S., 2011. Next-generation plate-tectonic reconstructions using GPlates. In: Geoinformatics, pp. 95–114.

Butler, R.F., 1992. Paleomagnetism: Magnetic Domains to Geologic Terranes. Blackwell Scientific Publications, Boston.

Buttau, C., Funedda, A., Pasci, S., Carmignani, L., Oggiano, G., Sale, V., 2008. Deformazione polifasica della successione mesozoica e terziaria del Supramonte (Sardegna orientale). Rend. online Soc. Geol. Ital., Note Brevi 1, 40–42.

Capitanio, F.A., Goes, S., 2006. Mesozoic spreading kinematics: consequences for Cenozoic Central and Western Mediterranean subduction. Geophys. J. Int. 165, 804–816.

Caricchi, C., Cifelli, F., Sagnotti, L., Sani, F., Speranza, F., Mattei, M., 2014. Paleomagnetic evidence for a post-Eocene 90° CCW rotation of internal Apennine units: a linkage with Corsica–Sardinia rotation? Tectonics 33, 374–392.

Carosi, R., Frassi, C., Iacopini, D., Montomoli, C., 2005. Post collisional transpressive tectonics in northern Sardinia (Italy). J. Virtual Explorer 19. paper 3.

Chabrier, G., Fourcade, E., Jaffrezo, M., 1975. Sur le Crétacé du Sud-Ouest de la Sardegne. Bull. Soc. Géol. Fr., 131–134.

Cherchi, A., 1985. Guidebook to the 19th European Micropaleontological Colloquium, Sardinia. AGIP, p. 340.

Cherchi, A., Mancin, N., Montadert, L., Murru, M., Putzu, M.T., Schiavinotto, F., Verrubbi, V., 2008. The stratigraphic response to the Oligo-Miocene extension in the western Mediterranean from observations on the Sardinia graben system (Italy). Bull. Soc. Géol. Fr. 179, 267–287.

Cherchi, A., Simone, L., Schroeder, R., Carannante, G., 2010. I sistemi carbonatici giurassico – cretacei della Nurra (Sardegna settentrionale). Geol. Field Trips 2, 55–123.

Cifelli, F., Mattei, M., 2010. Curved orogenic systems in the Italian Peninsula: a paleomagnetic review. J. Virtual Explorer 36. paper 17.

Cifelli, F., Mattei, M., Rossetti, F., 2007. Tectonic evolution of arcuate mountain belts on top of a retreating subduction slab: the example of the Calabrian Arc. J. Geophys. Res. 112, B09101. http://dx.doi.org/10.1029/2006JB004848.

Costamagna, L.G., Barca, S., Lecca, L., 2007. The Bajocian–Kimmeridgian Jurassic sedimentary cycle of eastern Sardinia: stratigraphic, depositional and sequence interpretation of the new "Baunei Group". C. R. Géosci. 339, 601–612.

Deenen, M.H.L., Langereis, C.G., van Hinsbergen, D.J.J., Biggin, A.J., 2011. Geomagnetic secular variation and the statistics of palaeomagnetic directions. Geophys. J. Int. 186, 509–520.

Dieni, I., Massari, F., 1963a. Il Cretaceo nei dintorni di Orosei (Sardegna). Accademia Nazionale dei Lincei, pp. 575–580.

Dieni, I., Massari, F., 1965. Le Crétacé inférieur d'Orosei (Sardaigne) et ses analogies avec celui du Sud-Est de la France. In: Colloque sur le Crétacé inférieur, Lyon, 1963. Mém. Bureau Rech. Géolog. Minières 34, 795–799.

Espurt, N., Hippolyte, J.-C., Saillard, M., Bellier, O., 2012. Geometry and kinematic evolution of a long-living foreland structure inferred from field data and cross section balancing, the Sainte-Victoire System, Provence, France. Tectonics 31, TC4021. http://dx.doi.org/10.1029/2011TC002988.

Faccenna, C., Becker, T.W., Pio Lucente, F., Jolivet, L., Rossetti, F., 2001a. History of subduction and back-arc extension in the Central Mediterranean. Geophys. J. Int. 145, 809–820.

Faccenna, C., Funiciello, F., Giardini, D., Lucente, P., 2001b. Episodic back-arc extension during restricted mantle convection in the Central Mediterranean. Earth Planet. Sci. Lett. 187, 105–116.

Faccenna, C., Piromallo, C., Crespo-Blanc, A., Jolivet, L., Rossetti, F., 2004. Lateral slab deformation and the origin of the western Mediterranean arcs. Tectonics 23.

Fisher, R.A., 1953. Dispersion on a sphere. Proc. R. Soc. Lond. A 217, 295–305.

Frisch, W., 1979. Tectonic progradation and plate tectonic evolution of the Alps. Tectonophysics 60, 121–139.

Gaina, C., Roest, W.R., Müller, R.D., 2002. Late Cretaceous–Cenozoic deformation of northeast Asia. Earth Planet. Sci. Lett. 197, 273–286.

Gaina, C., Torsvik, T.H., van Hinsbergen, D.J.J., Medvedev, S., Werner, S.C., Labails, C., 2013. The African Plate: a history of oceanic crust accretion and subduction since the Jurassic. Tectonophysics 604, 4–25.

Gattacceca, J., Deino, A.L., Rizzo, R., Jones, B., Henry, B., Beaudoin, B., Vadeboin, F., 2007. Miocene rotation of Sardinia: new paleomagnetic and geochronological constraints and geodynamic implications. Earth Planet. Sci. Lett. 258, 359–377.

Gong, Z., Langereis, C.G., Mullender, T.A.T., 2008. The rotation of Iberia during the Aptian and the opening of the Bay of Biscay. Earth Planet. Sci. Lett. 273, 80–93.

Gong, Z., van Hinsbergen, D.J.J., Dekkers, M.J., 2009. Earth Planet. Sci. Lett. 284, 292–301.

Gradstein, F.M., Ogg, J.G., Schmitz, M., Ogg, G., 2012. The Geologic Time Scale 2012. Elsevier, Amsterdam.

Handy, M.R., Schmid, S.M., Bousquet, R., Kissling, E., Bernoulli, D., 2010. Reconciling plate-tectonic reconstructions of Alpine Tethys with the geological–geophysical record of spreading and subduction in the Alps. Earth-Sci. Rev. 102, 121–158.

Heymes, T., Monié, P., Arnaud, N., Pêcher, A., Bouillin, J.-P., Compagnoni, R., 2010. Alpine tectonics in the Calabrian–Peloritan belt (southern Italy): new $^{40}Ar/^{39}Ar$ data in the Aspromonte Massif area. Lithos 114, 451–472.

Horner, F., Lowrie, W., 1981. Paleomagnetic evidence from Mesozoic carbonate rocks for the rotation of Sardinia. J. Geophys 49 (1), 11–19.

Johnson, C.L., Constable, C.G., Tauxe, L., Barendregt, R., Brown, L.L., Coe, R.S., Layer, P., Mejia, V., Opdyke, N.D., Singer, B.S., Staudigel, H., Stone, D.B., 2008. Recent investigations of the 0–5 Ma geomagnetic field recorded by lava flows. Geochem. Geophys. Geosyst. 9, Q04032. http://dx.doi.org/10.1029/2007GC001696.

Jolivet, L., Faccenna, C., Piromallo, C., 2009. From mantle to crust: stretching the Mediterranean. Earth Planet. Sci. Lett. 285, 198–209.

Kirscher, U., Aubele, K., Muttoni, G., Ronchi, A., Bachtadse, V., 2011. Paleomagnetism of Jurassic carbonate rocks from Sardinia: no indication of post-Jurassic internal block rotations. 116, B12107. http://dx.doi.org/10.1029/2011JB008422.

Kirschvink, J.L., 1980. The least-squares line and plane and the analysis of palaeomagnetic data. Geophys. J. R. Astrol. Soc. 62, 699–718.

Lacombe, O., Jolivet, L., 2005. Structural and kinematic relationships between Corsica and the Pyrenees-Provence domain at the time of the Pyrenean orogeny. Tectonics 24.

Maffione, M., Speranza, F., Faccenna, C., Cascella, A., Vignaroli, G., Sagnotti, L., 2008. A synchronous Alpine and Corsica–Sardinia rotation. J. Geophys. Res. 113, B03104. http://dx.doi.org/10.1029/2007JB005214.

Maffione, M., Speranza, F., Cascella, A., Longhitano, S.G., Chiarella, D., 2013. A ∼125° post-early Serravallian counterclockwise rotation of the Gorgoglione Formation (Southern Apennines, Italy): new constraints for the formation of the Calabrian Arc. Tectonophysics 590, 24–37.

Malinverno, A., Ryan, W.B.F., 1986. Extension in the Tyrrhenian Sea and shortening in the Apennines as result of arc migration driven by sinking of the lithosphere. Tectonics 5, 227–245.

McFadden, P.L., 1990. A new fold-test for palaeomagnetic studies. Geophys. J. Int. 103, 163–169.

McFadden, P.L., McElhinny, M.W., 1988. The combined analysis of remagnetisation circles and direct observations in paleomagnetism. Earth Planet. Sci. Lett. 87, 161–172.

Müller, R.D., Royer, J.-Y., Cande, S.C., Roest, W.R., Maschenkov, S., 1999. New constraints on the Late Cretaceous/Tertiary plate tectonic evolution of the Caribbean. Sediment. Basins World 4, 33–59.

Murru, M., Salvadori, A., 1990. Ricerche stratigrafiche sul bacino paleogenico del Sulcis (Sardegna sud-occidentale). Geologica Rom. 26 (1987), 149–165.

Muttoni, G., Lanci, L., Argnani, A., Hirt, A.M., Cibin, U., Abrahamsen, N., Lowrie, W., 2000. Paleomagnetic evidence for a Neogene two-phase counterclockwise tectonic rotation in the Northern Apennines (Italy). Tectonophysics 326, 241–253.

Olivet, J.L., 1996. Kinematics of the Iberian Plate. Bull. Cent. Rech. Explor. 20, 131–195.

Raponi, D., 2003. Studio paleontologico-stratigrafico di successioni paleogeniche della Sardegna centro-meridionale. PhD thesis. Univ. Modena, Reggio Emilia, pp. 1–175.

Rosenbaum, G., Lister, G.S., 2004. Neogene and Quaternary rollback evolution of the Tyrrhenian Sea, the Apennines, and the Sicilian Maghrebides. Tectonics 23.

Rosenbaum, G., Lister, G.S., Duboz, C., 2002a. Relative motions of Africa, Iberia and Europe during Alpine orogeny. Tectonophysics 359, 117–129.

Rosenbaum, G., Lister, G.S., Duboz, C., 2002b. Reconstruction of the tectonic evolution of the western Mediterranean since the Oligocene. J. Virtual Explorer 8, 107–130.

Rossetti, F., Goffé, B., Monié, P., Faccenna, C., Vignaroli, G., 2004. Alpine orogenic P-T-t-deformation history of the Catena Costiera area and surrounding regions (Calabrian Arc, southern Italy): the nappe edifice of north Calabria revised with insights on the Tyrrhenian–Apennine system formation. Tectonics 23.

Ruiz-Martinez, V.C., Torsvik, T.H., van Hinsbergen, D.J.J., Gaina, C., 2012. Earth at 200 Ma: global palaeogeography refined from CAMP palaeomagnetic data. Earth Planet. Sci. Lett. 331–332, 67–79.

Savostin, L.A., Sibuet, J.C., Zonenshain, L.P., Le Pichon, X., Roulet, M.-J., 1986. Kinematic evolution of the Tethys belt from the Atlantic Ocean to the Pamirs since the Triassic. Tectonophysics 123, 1–35.

Schmid, S.M., Fügenschuh, B., Kissling, E., Schuster, R., 2004. Tectonic map and overall architecture of the Alpine orogen. Eclogae Geol. Helv. 97 (1), 93–117.

Séranne, M., 1999. The Gulf of Lion continental margin (NW Mediterranean) revisited by IBS: an overview. In: Special Publications, vol. 156. Geological Society, London, pp. 15–36.

Sibuet, J.C., Srivastava, S.P., Spakman, W., 2004. Pyrenean orogeny and plate kinematics. J. Geophys. Res. 109, B08104. http://dx.doi.org/10.1029/2003JB002514.

Simone, L., Cherchi, A., 2009. The Cretaceous carbonate system of the Nurra region (North Western Sardinia, Italy). In: IAS 2009, 27th Meeting, field trip 11. ISBN 978-88-7587-554-1, pp. 223–234.

Speranza, F., Villa, I.M., Sagnotti, L., Florindo, F., Cosentino, D., Cipollari, P., Mattei, M., 2002. Age of the Corsica–Sardinia rotation and Liguro-Provençal Basin spreading: new paleomagnetic and Ar/Ar evidence. Tectonophysics 347, 231–251.

Speranza, F., Minelli, L., Pignatelli, A., Chiappini, M., 2012. The Ionian Sea: the oldest in situ ocean fragment of the world? J. Geophys. Res. 117, B12101. http://dx.doi.org/10.1029/2012JB009475.

Stampfli, G.M., Hochard, C. (Eds.), 2009. Plate Tectonics of the Alpine Realm. Special Publications, vol. 327. Geological Society, London, pp. 89–111.

Stampfli, G.M., Borel, G.D., Marchant, R., Mosar, J., 2002. Western Alps geological constraints on western Tethyan reconstructions. J. Virtual Explorer 08.

Tauxe, L., 2005. Inclination flattening and the geocentric axial dipole hypothesis. Earth Planet. Sci. Lett. 233, 247–261.

Tauxe, L., Butler, R.F., Van der Voo, R., Banerjee, S.K., 2010. Essentials of Paleomagnetism. University of California Press, Berkeley, ISBN 978-0-520-26031-3. 489 pp.

Torsvik, T.H., Van der Voo, R., Preeden, U., Mac Niocaill, C., Steinberger, B., Doubrovine, P.V., van Hinsbergen, D.J.J., Domeier, M., Gaina, C., Tohver, E., Meert, J.G., McCausland, P.J.A., Cocks, L.R.M., 2012. Phanerozoic polar wander, paleogeography and dynamics. Earth-Sci. Rev. 114, 325–368.

Trémolières, P., Cherchi, A., Schroeder, R., 1984. Pyrenean thrust faulting in the Mesozoic of NW Sardinia. C. R. Acad. Sci., Ser. II 18, 797–800.

Turco, E., Macchiavelli, C., Mazzoli, S., Schettino, A., Pierantoni, P.P., 2012. Kinematic evolution of Alpine Corsica in the framework of Mediterranean mountain belts. Tectonophysics 579, 193–206.

Van der Voo, R., 1969. Paleomagnetic evidence for the rotation of the Iberian Peninsula. Tectonophysics 7, 5–56.

van Hinsbergen, D., Vissers, R., Spakman, W., 2014. Origin and consequences of western Mediterranean subduction, rollback, and slab segmentation. Tectonics 33 (4), 393–419.

Vigliotti, L., Alvarez, W., McWilliams, M., 1990. No relative rotation detected between Corsica and Sardinia. Earth Planet. Sci. Lett. 98, 313–318.

Vigliotti, L., Kent, D.V., 1990. Paleomagnetic results of Tertiary sediments from Corsica: evidence of post-Eocene rotation. Phys. Earth Planet. Inter. 62, 97–108.

Vissers, R.L.M., Meijer, P.T., 2012a. Iberian plate kinematics and Alpine collision in the Pyrenees. Earth-Sci. Rev. 114, 61–83.

Vissers, R.L.M., Meijer, P.T., 2012b. Mesozoic rotation of Iberia: subduction in the Pyrenees? Earth-Sci. Rev. 110, 93–110.

Vissers, R., van Hinsbergen, D., Meijer, P.T., 2013. Kinematics of Jurassic ultra-slow spreading in the Piemonte Ligurian ocean. Earth Planet. Sci. Lett. 380, 138–150.

Wiedmann, J., Dieni, I., 1968. Die Kreide Sardiniens und ihre Cephalopoden. Paleontogr. Ital. 64, 1–171.

Zijderveld, J.D.A., 1967. A. C. demagnetization of rocks: analysis of results. In: Methods in Palaeomagnetism. Elsevier, Amsterdam, New York, pp. 254–286.